Bacterial Swimming Strategies and Turbulence

Rolf H. Luchsinger,*# Birger Bergersen,# and James G. Mitchell§

*Theoretical Methods CCRC.C4, ABB Corporate Research LTH, CH-5405 Bade-Daetwill, Switzerland; #Department of Physics and Astronomy, University of British Columbia, Vancouver, British Columbia V6T 1Z1, Canada; and §Biological Sciences, Flinders University, Adelaide SA 5001, Australia

ABSTRACT Most bacteria in the ocean can be motile. Chemotaxis allows bacteria to detect nutrient gradients, and hence motility is believed to serve as a method of approaching sources of food. This picture is well established in a stagnant environment. In the ocean a shear microenvironment is associated with turbulence. This shear flow prevents clustering of bacteria around local nutrient sources if they swim in the commonly assumed "run-and-tumble" strategy. Recent observations, however, indicate a "back-and-forth" swimming behavior for marine bacteria. In a theoretical study we compare the two bacterial swimming strategies in a realistic ocean environment. The "back-and-forth" strategy is found to enable the bacteria to stay close to a nutrient source even under high shear. Furthermore, rotational diffusion driven by thermal noise can significantly enhance the efficiency of this strategy. The superiority of the "back-and-forth" strategy suggests that bacterial motility has a control function rather than an approach function under turbulent conditions.

INTRODUCTION

Bacteria constitute an essential part of the food web in the ocean (Azam, 1998). They efficiently recycle dissolved organic carbon (DOC) exuded by other organisms such as algae. They feast on organic matter produced when a dying cell lyses or from waste material when predation takes place. Marine bacteria are also an important food source for flagellates, and they play an important role in the life cycles of a number of viruses (Hennes and Suttle, 1995).

While most marine bacteria are capable of motility, it is used only intermittently. Their swimming speed can reach more than 100 body lengths per second (Mitchell et al., 1996), suggesting that motility is important for some of the environmental niches that marine bacteria occupy.

It is generally accepted that bacterial motion is controlled by some form of chemotaxis. In the case of enteric bacteria, such as *Escherichia coli*, Berg and Brown (1974) were able to give a detailed model of the chemotaxis. According to the so-called run-and-tumble (or twiddle) strategy, bacteria swim at a constant speed, stop after a while, then tumble and continue in a random direction. To be able to approach a high-nutrient environment, the run times must be biased. If the rate of nutrient uptake is increasing, as it would be if the bacterium swims toward a nutrient-rich region, the run time is on average increased over the mean run time. The run-and-tumble model successfully explains the behavior of *E. coli.*

However, turning our attention away from enteric bacteria and toward bacteria in the open ocean, one has to face the problem of turbulence. Energy flow into the ocean due to wind, convection, and gravitational forces leads to complex water movements. These flows affect the physics of the ocean down to the micrometer scale, where they can be described by shear flows. Here we will consider bacteria attempting to cluster around localized sources of nutrient, such as phytoplankton exuding organic molecules. Recently, Bowen et al. (1993) simulated the bacterial clustering around phytoplankton cells in a turbulent ocean. In the absence of a chemotaxis model for marine bacteria, they adapted the run-and-tumble model of Brown and Berg (1974). While clustering was found at low shear, the fraction of a bacterial population that clustered around the nutrient patch was insignificant for higher shear. This suggests that the run-and-tumble strategy is not well suited for a turbulent environment. Indeed, a motility behavior different from that of *E. coli* has been found in some marine bacteria. The aerotactic swimming behavior of marine bacteria near air bubbles (Mitchell et al., 1996) and in thin sheets near sediment layers (Barbara and Mitchell, 1996) was recently studied. While the basic stop-and-go pattern was the same as in the run-and-tumble model of *E. coli*, there were two major differences. First, the velocity of the marine bacteria was variable and could reach 200 μm s^{-1}, which is an order of magnitude faster than the velocity of enteric bacteria. Second, instead of tumbling the marine bacteria simply reversed their direction after each stop. Thus, these marine bacteria employed a back-and-forth rather than a run-and-tumble strategy. This behavior has also been seen around localized nutrient patches (Barbara and Blackburn, private communications).

The central question is whether these differences in motility are related to the differences in the physical environment. The purpose of this work is to compare the effectiveness of the back-and-forth and the run-and-tumble strategies under oceanic flow conditions.

THE MODEL

The building blocks of our model are algae, the nutrient exuded by algae, bacteria, and the velocity field of the ocean water surrounding the particles.

Received for publication 5 January 1999 and in final form 28 July 1999.

Address reprint requests to Dr. Birger Bergersen, Department of Physics and Astronomy, University of British Columbia, Vancouver, BC V6T 1Z1, Canada. Tel.: 604-822-2754; Fax: 604-822-5324; E-mail: birger@physics.ubc.ca.

0006-3495/99/11/2377/10 $2.00

The focus of our study is on the vicinity of an alga, where the concentration of exuded DOC is high compared to background. On this small length scale, significant simplifications of the flow velocity field can be made. The algae exude nutrient, which diffuses away and is advected by the flow. In the steady state a nutrient-rich region is established close to the alga. Its form depends on the flow pattern. It is this nutrient-rich region rather than the source itself that is important to the bacteria. The chemotactic response to changes in the DOC concentration then enables the bacteria to locate the nutrient-rich zone.

Ocean turbulence at the bacterial scale

Oceanic turbulence covers many length scales. It is therefore important to be aware of the typical length scale of the problem at hand. In our model, the dimension of a bacterium is in the 0.1–1 μm range, while the size of an alga is on the order of 10 μm. The speed of a marine bacterium is on the order of 100 μm s^{-1}, and the typical run time is ~1 s. Therefore, the length scale of the problem is on the order of a few hundred micrometers. The Kolmogorov length is given by $(\nu^3/\epsilon)^{1/4}$, where ν is the kinematic viscosity and ϵ is the viscous energy dissipation rate. This length varies between ~1 and 6 mm in the ocean (Lazier and Mann, 1989). The Kolmogorov scale is considered to be a measure of the length scale of the smallest eddies in a fluid, although the exact relation is still under debate (Lazier and Mann, 1989; Hill et al., 1992; Mitchell et al., 1985). Our problem is well below that scale, and the fluid velocity field thus can be linearized (Batchelor, 1980).

The motion of phytoplankton in the ocean may be quite complicated. Some species are motile, and buoyancy can lead to motion relative to the surrounding fluid. To make the problem tractable, however, we assume algae to be passive. A 10-μm-diameter alga that is not swimming will have a settling speed on the order of 1 μm s^{-1}. This velocity is small compared to bacterial swimming velocities. As has been argued (Bowen et al., 1993), the nutrient distribution around an alga of this size will not be strongly affected by the settling motion between the alga and the surrounding fluid for the shear rates considered here, and it is reasonable to set the center of reference of the simulations at the position of an alga. The fluid velocity field $\mathbf{u}(\mathbf{x})$ relative to the alga can thus be written in the linear form

$$\mathbf{u}(\mathbf{x}) = \mathbf{G}\mathbf{x}, \tag{1}$$

where $\mathbf{G}$ is the velocity gradient tensor and $\mathbf{x}$ is the position vector relative to the position of the alga.

It is common practice to split the velocity gradient tensor $\mathbf{G}$ into a symmetrical and an antisymmetrical part,

$$\mathbf{G} = \mathbf{E} + \mathbf{\Omega}, \tag{2}$$

with

$$E_{ij} = \tfrac{1}{2}(G_{ij} + G_{ji}), \tag{3}$$

$$\Omega_{ij} = \tfrac{1}{2}(G_{ij} - G_{ji}). \tag{4}$$

The symmetrical part $\mathbf{E}$ is called the rate-of-strain tensor and describes shearing of the fluid. The antisymmetrical part $\mathbf{\Omega}$ describes the vorticity of the fluid. To have incompressible flow, $\mathbf{G}$ must be traceless. By definition all of the diagonal elements of $\mathbf{\Omega}$ vanish, and therefore the constraint of incompressible flow implies that the diagonal elements of $\mathbf{E}$ add to zero.

Because $\mathbf{E}$ is symmetrical it can be diagonalized by a rotation of the coordinate system. Together with the constraint of incompressibility we are left with two parameters to define $\mathbf{E}$. Ordering the three elements $E_1 \geq E_2 \geq E_3$ of the diagonalized rate-of-strain tensor, the two parameters are defined by (Bowen and Stolzenbach 1992)

$$E_b = \frac{1}{2}\sum_{i=1}^{3}|E_i|, \tag{5}$$

$$\gamma = \frac{2E_2}{E_b} \quad (-1 \leq \gamma \leq 1), \tag{6}$$

where E_b specifies the strength of the shearing and γ is a symmetry factor. Reversing these expressions, we can write

$$\begin{aligned} E_1 &= E_b(1 - \tfrac{1}{4}(\gamma + |\gamma|)), & E_1 &> 0, \\ E_2 &= E_b\frac{\gamma}{2}, & E_1 &\geq E_2 \geq E_3, \\ E_3 &= -E_b(1 + \tfrac{1}{4}(\gamma - |\gamma|)), & E_3 &< 0. \end{aligned} \tag{7}$$

For negative values of γ, there is incoming flow in two directions and outgoing flow in one direction, for positive γ outgoing flow in two directions. For $\gamma = 0$, the shear flow vanishes in the y direction.

The viscous energy dissipation rate ϵ is determined by the rate-of-strain tensor (Batchelor 1987):

$$\epsilon = \frac{1}{2}\nu\sum_{i,j}\left(\frac{\partial u_i}{\partial x_j} + \frac{\partial u_j}{\partial x_i}\right)^2 = 2\nu\sum_{i,j}E_{ij}^2 = 2\nu E_b^2\left(2 + \frac{\gamma^2}{2} - |\gamma|\right). \tag{8}$$

Therefore, the magnitude of the rate-of-strain tensor is given largely by the viscous energy dissipation rate, which in the ocean mainly takes on values ranging from $\epsilon = 10^{-1}$ cm^2 s^{-3} near the surface under strong wind forcing (Denman and Gargett 1995) to $\epsilon = 10^{-6}$ cm^2 s^{-3} at the thermocline (Denman and Gargett 1988). According to Eq. 8 the strength of the rate-of-strain tensor ranges from about $E_b = 1.5$ s^{-1} at the upper mixed layer to low values of $E_b = 0.005$ s^{-1} at the thermocline.

Thus a small enough particle in a turbulent flow sees a velocity field varying linearly in space and randomly in time with a typical spatial gradient on the order of $(\epsilon/\nu)^{1/2}$ and a time scale for the variation on order of the Kolmogorov time $(\nu/\epsilon)^{1/2}$ (Jiménez 1997). To have a tractable model, we consider the flow as static and compare the behavior of the bacteria under different flow conditions. While this approach is safe for low shear, where the Kolmogorov time is on the order of a minute, the Kolmogorov time can be on the order of a second for high shear. Because this can be compared to the run time of the bacteria, nonstationarity of the shear field might be expected to be important in this regime. Although we do not have a detailed model for the time dependence of the shear, toward the of the paper we will estimate the effect. We find, somewhat surprisingly perhaps, that even for shear as high as $E_b = 0.3$ s^{-1}, nonstationarity of E_b and γ does not alter our main findings. Furthermore, the dissipation rate is intermittent, and hence the mean value of ϵ may be much larger than the median (Baker and Gibson, 1987). However, events with very high energy dissipation rates are rare (Jiménez, 1997) and thus are not considered here.

We will find that the efficiency of the back-and-forth bacterial swimming strategy depends on the shear symmetry factor γ, but the distribution of γ-values appears not to have been studied in a natural environment. By numerical simulation Ashurst et al. (1987) found that the mean value of γ increased from almost zero to a value of 0.5 as ϵ was increased. Thus we will use $\gamma = 0.5$ as a typical value in our simulations.

We have found no references to typical values of the vorticity in a natural environment. It seems reasonable to assume that the strength of $\mathbf{\Omega}$ is on the same order as E_b. The effect of shear is to transport a bacterium to and from its nutrient patch, while we intuitively expect the effect of $\mathbf{\Omega}$ to be neutral. In most of our simulations we neglect $\mathbf{\Omega}$, but we will also report some test simulations with nonzero vorticity which indicate that vorticity does not appear to change the basic picture.

Because of the finite size of the alga, the linear flow field of Eq. 1 has to be corrected for the flow to vanish at the surface of the alga. Assuming a spherical alga of radius a, the corrected flow field is given by (Batchelor

1980)

$$\mathbf{u}(\mathbf{x}) = \mathbf{E}\mathbf{x} + \left\{ -\frac{a^5}{r^5}\mathbf{I} - \frac{5a^3}{2r^3}\left(1 - \frac{a^2}{r^2}\right)\frac{\mathbf{x}\mathbf{x}}{r^2} \right\}\mathbf{E}\mathbf{x} + \mathbf{\Omega}\mathbf{x}, \quad (9)$$

with $r = |\mathbf{x}|$. The leading term of the correction is proportional to $(a/r)^3$ and is only important close to the surface of the alga.

Nutrient distribution around an alga

The nutrient distribution around a leaking alga depends on the surrounding flow. The present simulation is concerned with comparing different swimming strategies, not with calculating the absolute value of the nutrient uptake. For this reason it is not as important to know the nutrient concentration accurately as it is to understand the effect of the flow field and swimming motion on the residence time near a nutrient source. We assume that the alga exudes nutrient at a constant rate. Analytical solutions exist for the advection-diffusion equation with linear symmetrical flow for an initial delta-distributed density (Konopka 1995). Based on these results, the nutrient distribution around a point source exuding at a constant rate F is given by the time integral (Bowen and Stolzenbach, 1992; Batchelor, 1979)

$$C(\mathbf{x}, t) = \frac{F}{(2\pi D)^{3/2}} \int_{t_0}^{t} \prod_{i=1}^{3} \left[\sqrt{\frac{E_i}{\exp(2E_i t') - 1}} \exp\left(-\frac{1}{2D} \frac{E_i x_i^2}{\exp(2E_i t') - 1} \right) \right] dt', \quad (10)$$

where the E_i are the eigenvalues of the rate-of-strain tensor as given in Eq. 7 and D is the diffusion constant. The effect of vorticity is neglected. For $|\gamma| = 1$ we have derived analytical solutions for this integral, which are given in the Appendix. For a general value of γ the integral has to be solved numerically. We use the numerical results in all of our simulations to exploit the whole range of possible shear patterns. However, an important result from the analytical solutions is that the distribution approaches a steady state in a time inversely proportional to the shear strength E_b and is reached in a few seconds for shear values of the upper mixed layer of the ocean. Therefore we only consider steady-state distributions. For $\gamma = -1$, there is incoming flow in two directions and outgoing flow in one direction. Thus the spherical distribution without flow is compressed in two directions and expanded in one direction, forming a tube. Similarly, the incoming flow in one direction and outgoing flow in two directions for $\gamma = +1$ forms a disk.

The nutrient distribution determined by Eq. 10 is correct only under the assumption that the flow field around the alga is linear. This applies only if the alga is a point source. However, under typical conditions the size of the algae is much smaller than $\sqrt{D/E_b}$, which can be viewed as the size of the diffusive core of the nutrient distribution. Because the nutrient distribution within the diffusive core is dominated by diffusion rather than advection, finite size corrections of the flow field in this region have a small impact on the nutrient distribution and can therefore be neglected.

Chemotaxis

In the model for bacterial chemotaxis (Brown and Berg, 1974), the bacteria move in a stop-and-go mode, with a duration of a run on the order of a second. After a stop, the new direction of a bacterium is given by chance. To approach a favorable environment, the probability P_t that the run ends within the time interval Δt is reduced when it moves toward the favorable environment. Thus the bacterium moves in a biased random walk (run-and-tumble).

P_t is given by (Jackson, 1987)

$$P_t = \frac{\Delta t}{\tau}, \quad (11)$$

where τ is the run time and is determined by

$$\tau = \tau_0 \exp\left(\alpha \overline{\frac{dP_b}{dt}} \right), \quad (12)$$

$$\overline{\frac{dP_b}{dt}} = \tau_m^{-1} \int_{-\infty}^{t} \frac{dP_b}{dt'} \exp\left(\frac{(t' - t)}{\tau_m} \right) dt', \quad (13)$$

$$\frac{dP_b}{dt} = \frac{K_D}{(K_D + C)^2} \frac{dC}{dt}, \quad (14)$$

where τ_0 is the average run length, τ_m is the adaption time scale of the bacterial system, α is a chemotaxis sensitivity factor, $\overline{dP_b/dt}$ is the weighted rate of change of the fraction of a cellular protein surface receptor bound by the substrate, K_D is the half-saturation constant, and C is the concentration of the chemical to which the bacterium is sensitive.

The run-and-tumble model was established by investigating the chemotaxis of the enteric bacterium *E. coli.* No detailed chemotaxis model exists for bacteria that lack the tumble phase and instead reverse direction after each stop. We therefore assume that the run time is biased according to Eqs. 11–14 for marine bacteria as well.

Change of orientation

Small particles in water cannot move in a straight line. Collision with water molecules gives rise to random forces and torques. The most important in our case will be the random torques causing rotational diffusion. The corresponding diffusion constant is (Berg, 1983)

$$D_r = \frac{kT}{f_r}, \quad (15)$$

where k is the Boltzmann constant, T is the absolute temperature, and f_r is the rotational friction drag coefficient. For a sphere of radius a, f_r is given by

$$f_r = 8\pi\mu a^3, \quad (16)$$

where μ is the viscosity. Because D_r depends on the inverse cube of the radius of the particle, rotational diffusion prevents small bacteria from moving in a fixed direction. The relationship between D_r and the shape of the bacteria is not simple, mainly because of the flagellum (Mitchell, 1991). Hence we consider D_r to be determined by the effective size of a bacterium.

The orientation of the bacterium is affected not only by rotational diffusion, but also by the flow field. We propose that the velocity gradient in the flow will cause an elongated structure of linear dimension **d** to change its orientation according to

$$\frac{d\mathbf{e}_d}{dt} = \mathbf{e}_d \times \mathbf{G}\mathbf{e}_d \times \mathbf{e}_d, \quad (17)$$

where $\mathbf{e}_d$ is a unit vector in the direction of the object and **G** is the velocity gradient tensor of Eq. 1. A similar expression is given in section 2.2 in the review article by Pedley and Kessler (1992; see Eq. 2.4 in that paper). Our treatment differs from theirs in that we neglect any viscous torque $\mathbf{L}_v$ associated with the rotation of the flagellum. We also have assumed that the asymmetry factor α_0 of Pedley and Kessler is unity, i.e., that the flagellum is much longer than any linear dimension of the cell body.

Note that the change in orientation depends on the orientation relative to the flow but is independent of the linear dimension of the object. We call this effect rotational advection.

For bacteria, we set $\mathbf{e}_d$ equal to the swimming direction, with the flagellum forming the oblong structure. The effect of rotational advection in a pure symmetrical flow (pure shear) is to turn the bacteria into the direction of the outgoing flow. In pure rotational flow, bacteria will rotate with the ambient fluid.

Rotational advection is proportional to the magnitude of the velocity gradient tensor. Even for the highest shear values considered, the change in the swimming direction will not be large in a typical run of 1 s. Rotational advection is not important for bacteria employing the run-and-tumble strategy; because the heading direction is chosen randomly after each stop, any directed rotation due to rotational advection will be lost after each stop. In the back-and-forth strategy, however, the directed rotations of all of the runs add up (Fig. 1). Rotational advection changes the heading direction parallel to the outgoing flow. Going back and forth and parallel to the x direction, the bacterium is first advected toward the alga and then moves back and forth across the nutrient-rich region. This motility behavior is ideal in the sense that the effect of the flow in pushing the bacterium away from the alga is neutralized by going back and forth. Because of rotational advection in combination with the back-and-forth strategy, the bacterium can stay in the nutrient-rich region for a long time and therefore increase its nutrient uptake.

A bacterium passively drifting with the fluid follows one of the stream lines. Even if it passes close enough to traverse the nutrient-rich region, it will soon be swept away by the flow. From these general considerations it seems that the back-and-forth strategy for bacterial swimming is best adapted to the environment associated with turbulence. We further quantify this statement with simulations.

Simulation procedure

We assume an algal concentration (Sournia, 1978) of 1 cell mm^{-3} and take our simulation volume to be a sphere of radius $r_s = 620$ μm centered around an alga. A flow field is specified for the simulation volume. In most of our simulations we neglect vorticity and assume values for the parameters E_b and γ. A bacterium is randomly placed at the surface of the simulation volume with a random initial direction. The velocity of the bacterium relative to the alga $\mathbf{v}_r$ is the superposition of the bacterial swimming speed $\mathbf{v}$ and the flow field $\mathbf{u}$ from Eq. 9:

$$\mathbf{v}_r = \mathbf{u} + \mathbf{v}. \tag{18}$$

After each time interval Δt, the position of the bacterium is updated and the nutrient density C is computed from Eq. 10 at the new position. The four constants D, F, α and K_D can be combined into the normalized exudation rate F_*, defined as (Bowen et al., 1993)

$$F_* = \frac{F\alpha}{4\pi D K_D}. \tag{19}$$

Unless otherwise noted, we use $F_* = 1140$ μm s in our simulations. We fix F at 3.9×10^7 molecules s^{-1}. The half-saturation constant K_D is then given by specifying α and D.

The probability that the bacterium will stop within the next time interval follows from Eq. 11. A uniformly distributed random number R between 0 and 1 is picked, and if $P_t > R$, the run stops and a new swimming direction is chosen, either randomly (run-and-tumble) or by reversing the direction (back-and-forth). To take the response latency of the bacterium into account, the minimum run time was set at a fixed value τ_{min}. If the bacterium leaves the simulation volume, it is put back on the surface of this volume with random initial conditions. The radius of an alga a was set at 10 μm. If during the time interval Δt the bacterium collides with the alga, the move is rejected and a new random swimming direction is selected. No sticking at the alga is allowed. To obtain a reasonable statistic, one simulation is generally run for the simulation time $\tau_s = 36{,}000$ s. At each time step the swimming direction is also updated. Rotational diffusion leads to a change in the heading direction (Berg, 1983) of $\Delta\phi_d = (4D_r\Delta t)^{1/2}$. This change is accomplished by rotating the swimming direction of the bacterium around

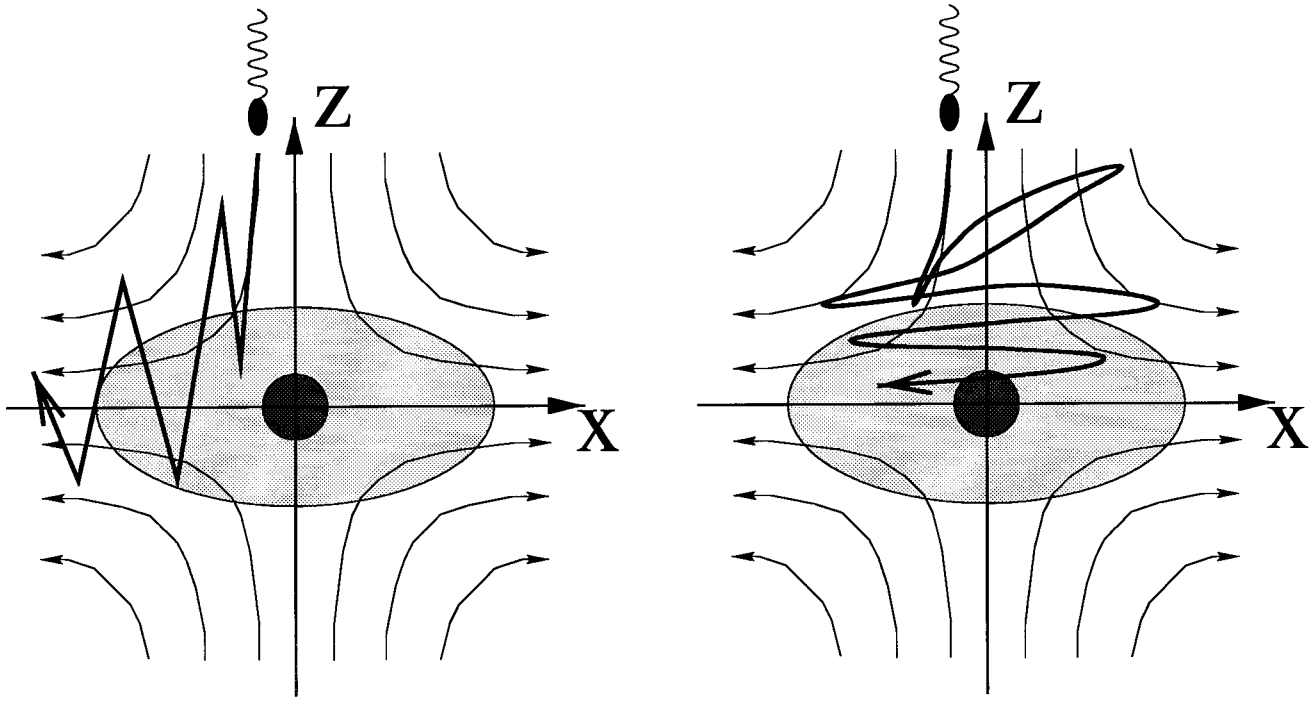

FIGURE 1 The motion of a back-and-forth bacterium in a pure shear fluid field around an alga, without rotational diffusion. The dark circle in the center represents the alga, and the shadow ellipse represents the region of high nutrient concentration around the alga, determined under shear. Without rotational advection (*A*) the heading direction is just reversed. The bacterium traverses the nutrient-rich region around the alga (*shaded region*) several times, but is advected away from the alga by the flow. The effect of rotational advection is shown in *B*.

a random axis normal to the original direction. For rotational advection, the swimming direction has to be updated according to Eq. 17 with the time increment Δt. A summary of the parameter values used is given in Table 1.

RESULTS AND DISCUSSION

The behavior of marine bacteria close to an alga is simulated under various conditions to compare run-and-tumble with the back-and-forth strategy. Default values of the parameters are $E_b = 0.3\ s^{-1}$, $\gamma = 0.5$, $v = 150\ \mu m\ s^{-1}$, and $D_r = 0.5\ rad^2\ s^{-1}$. Thus, if not otherwise stated, these values are used in all of the simulations of this section.

In the back-and-forth mode with the trajectory projected onto the *x-z* plane, stops and reversals of the heading directions can be seen in Fig. 2. The noisy changes in the heading direction are due to rotational diffusion. The path leads to a close encounter with the alga at the center of the figure. The bacterium remains there for a while but will eventually leave the region (not shown). In most cases the bacterium just passes by, but once in a while, by chance, it can stabilize its trajectory in the vicinity of the alga. This retention never happened for the run-and-tumble strategy under the shear conditions at hand.

Fig. 3 depicts the distance of a bacterium to the alga as a function of time. Mostly a bacterium is on the order of r_s (the radius of the simulation volume) away from the alga for both strategies. This reflects the procedure that a bacterium leaving the simulation volume is placed back on the surface of this volume. In the run-and-tumble strategy (Fig. 3 *A*), the bacterium occasionally gets close to the alga, but is soon swept away. The plot for a nonswimming (passive) bacterium looked the same. Thus, under high shear, bacteria in the run-and-tumble mode have essentially the same statistical behavior as nonmotile bacteria. However, the situation is very different in the back-and-forth mode (Fig. 3 *B*). Once a bacterium comes close to the alga, it sometimes succeeds in staying there for a while. The bacterium may be "dancing" around the alga for minutes before it leaves.

Fig. 3 implies that bacteria can be viewed as being in one of two states, either far away from the alga or dancing around it. This separation makes it possible to define a distance, below which the bacterium is defined to be in a resident state. We define this distance r_n to be 100 μm (Fig. 3). At this distance, the nutrient density is ~1/10 of its maximum value at the surface of the alga. Thus the resident region also represents the nutrient-rich region around the alga. A residence time can then be defined as the time interval between the entrance of a bacterium into the nutrient-rich region and its departure.

TABLE 1 Model parameters and their values

Exudation rate, F	3.9×10^7 molecules s^{-1}
Normalized exudation rate, F_*	1140 μm s
Diffusion constant, D	1000 $\mu m^2\ s^{-1}$
Radius of the alga, a	10 μm
Bacterial swimming speed, v	0–150 $\mu m\ s^{-1}$
Chemotaxis sensitivity factor, α	660 s
Average run time, τ_0	1.0 s
Adaption time scale, τ_m	1.0 s
Response latency time, τ_{min}	0.2 s
Rotational diffusion coefficient, D_r	0.06–4.0 $rad^2\ s^{-1}$
Characteristic shear rate, E_b	0.0–0.3 s^{-1}
Shear symmetry factor, γ	−1.0–1.0
Radius of simulation region, r_s	620 μm
High nutrient region, r_n	100 μm
Simulation time, τ_s	36,000 s
Time interval, Δt	0.01 s

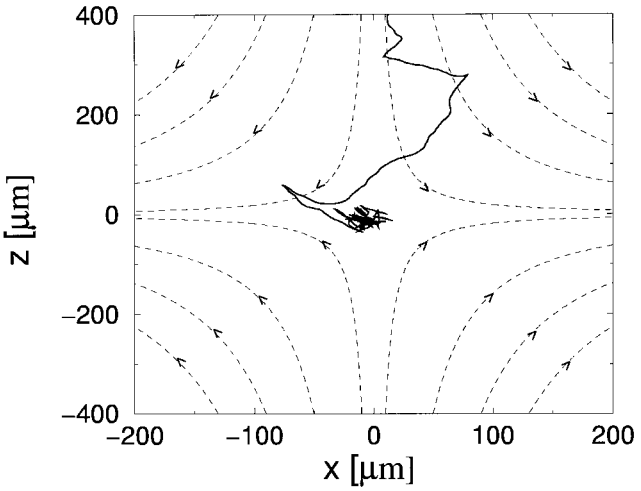

FIGURE 2 Simulated trajectory of a bacterium in the back-and-forth mode close to an alga. The projection on the *x-z* plane is shown.

From Fig. 3 it is obvious that the residence time varies from encounter to encounter. The statistics of the residence time is shown in Fig. 4. To obtain sufficient statistics, the simulation was run until the bacterium had made 18,000 visits. A visit was counted when it lasted for more than twice the average run time τ_0. The linear behavior in the log-linear plot indicates that the probability of a bacterium leaving the nutrient-rich region is independent of the time that it has already been there (Poisson process). Only for the shortest residence times is there a deviation from linear behavior.

To quantify the relative advantages of the different motility strategies, we assumed the bacterium to be a perfect, spherical nutrient absorber. Nutrient flux into the bacterium with radius a is then given by (Berg 1983)

$$I = 4\pi DaC, \tag{20}$$

where D is the diffusion constant and C is the nutrient concentration. The nutrient uptake of a bacterium is the integral of I over time along the trajectory of the bacterium. The nutrient gain is then defined as the ratio of the nutrient uptake of an active bacterium (in run-and-tumble or back-and-forth mode) to the nutrient uptake of a nonmotile bacterium under the same conditions.

One of the major findings of Mitchell et al. (1996) was that the speed of marine bacteria is higher than that of enteric bacteria. We investigated the influence of bacterial speed under high ($E_b = 0.3\ s^{-1}$) and low ($E_b = 0.05\ s^{-1}$)

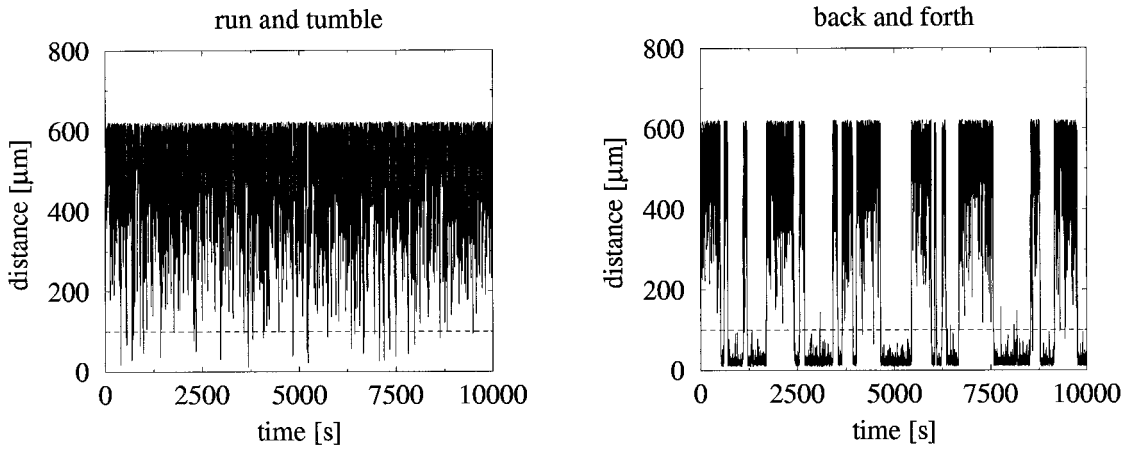

FIGURE 3 The distance of a bacterium from the alga as a function of time for high shear. While bacteria in the run-and-tumble mode cannot remain near the alga (*A*), significant residence times are possible in the back-and-forth strategy (*B*). The dashed line represents the boundary of the high-nutrient region as defined in the text.

shear on the nutrient gain (Fig. 5). The difference in nutrient gain for back-and-forth compared to run-and-tumble is striking for all shear rates and bacteria speeds. While a typical nutrient gain of a run-and-tumble bacterium is 3, the value can reach 200 for a bacterium in the back-and-forth mode. This difference reflects the fact that bacteria in the back-and-forth mode can stay longer in the high-nutrient region.

Different swimming speed dependencies are found for low and high shear. For low shear (Fig. 5 *A*), nutrient gain reaches a maximum at low speed and drops with increasing speed. At low shear rates, when ambient flow is almost zero, high speed leads to unnecessary movement away from the surface of the alga. Indeed, without an ambient flow, the best strategy for the bacterium once it has reached the alga would be to stop moving. For high shear (Fig. 5 *B*), nutrient gain increases with speed. However, there is a saturation at velocities beyond 50 μm s^{-1}, and we expect that for higher velocities the nutrient gain will drop.

In general, nutrient uptake decreases with increasing shear, because the nutrient-rich region becomes less localized and the residence time decreases. But as can be seen in Fig. 5, the nutrient gain is higher in the high shear case for swimming speeds above 100 μm s^{-1}. Thus the gain of the back-and-forth strategy (ratio of nutrient uptakes) becomes larger under high shear, while the actual uptake decreases.

Nutrient gain depends on both the speed of the bacterium and the shear (Fig. 6). Again, the nutrient gain is much higher for the back-and-forth than for the run-and-tumble strategy for all simulated shear conditions. In terms of the shear, the nutrient gain reaches a maximum at the intermediate rate $E_b = 0.15$ s^{-1} and drops for higher shear rates. This result indicates that neither the back-and-forth nor any other strategy will be very advantageous compared to a passive bacterium, as the shear reaches values orders of magnitude higher than those used here.

Considering the symmetry of the shear, nutrient gain is much higher for negative γ. Comparing the two extremes: $\gamma = -1$ means the flow away from the alga is parallel to the x axis, while $\gamma = 1$ leads to radial outflow in the x-y plane. Thus, rotational advection, which tends to align the bacterium parallel to the outgoing flow, is much more effective for $\gamma = -1$, because there is only one such direction. On the other hand, for $\gamma = 1$, there are in fact infinitely many different directions of the outgoing flow. Thus the bacterium will be turned in many different directions along its path, and there is no overall cumulative effect. For this reason the effect of rotational advection is much more pronounced for negative γ. Regarding the strength of the shear, rotational advection becomes more important for higher values of E_b, as expected. For vanishing shear, the effect of rotational advection vanishes.

The deterministic ordering effect of rotational advection can be spoiled by the stochastic rotational diffusion. Indeed,

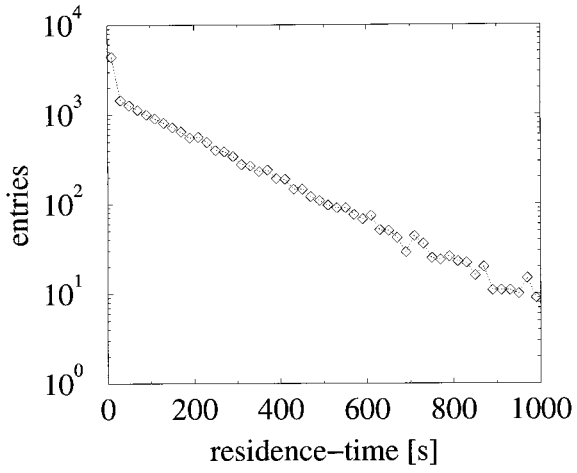

FIGURE 4 Histogram of the residence time for bacteria employing the back-and-forth strategy.

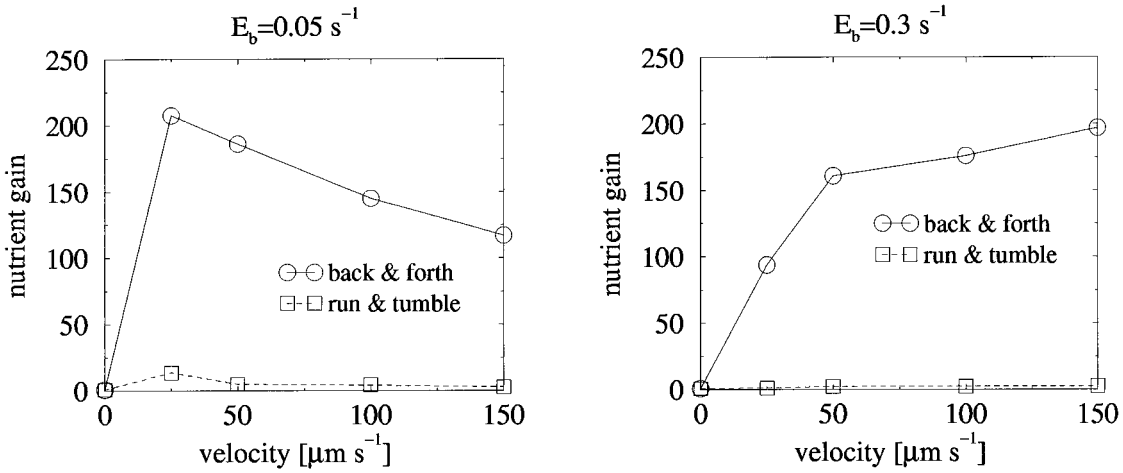

FIGURE 5 The nutrient gain of a bacterium as a function of its speed for low (*A*) and high (*B*) shear. Under both shear conditions, the nutrient gain for bacteria using the back-and-forth strategy is much higher than for bacteria using the run-and-tumble strategy.

for small bacteria, rotational diffusion can become dominant. To clearly demonstrate the effect of rotational advection, a small value for D_r was used in Fig. 6. The role of rotational diffusion is shown in Fig. 7, where the mean residence time is plotted against the rotational diffusion coefficient. A long residence time implies a long stay in the nutrient-rich region and therefore a high nutrient uptake. Thus the qualitative behaviors of residence time and nutrient gain are similar. But the residence time is a truly local entity. It just measures how long a bacterium stays on average in the nutrient-rich region once it is there. How it arrives there and what it does away from the alga are not considered.

The most intriguing feature of Fig. 7 is that there is an optimal level for D_r for some types of shear flow. Thus some level of orientational noise is helpful in making a long stay at the alga possible. Because a bacterium in our back-and-forth model has no way to change its heading direction actively, orientation is changed either by the flow (rotational advection) or by Brownian rotational diffusion. As shown in Fig. 1, a back-and-forth bacterium with a fixed heading will always be washed away from the alga by the flow. Thus the ability to change orientational direction seems crucial. For positive values of γ, rotational advection is less important, and the orientational change of a bacterium is dominated by rotational diffusion. Fig. 7 demonstrates that a certain amount of orientational change, even that due to rotational diffusion, helps to increase the residence time. On the other hand, if rotational diffusion becomes too strong, the bacterial trajectory becomes erratic and residence time decreases.

For intermediate values of D_r, the residence time for $\gamma = 0.5$ is about twice the time for $\gamma = -1.0$. The reason for this is that the outgoing flow along a particular direction has twice the magnitude for $\gamma = -1.0$ than for $\gamma = 1.0$. Because the flow is the factor limiting residence time, the higher flow for $\gamma = -1.0$ leads to shorter residence times. Resi-

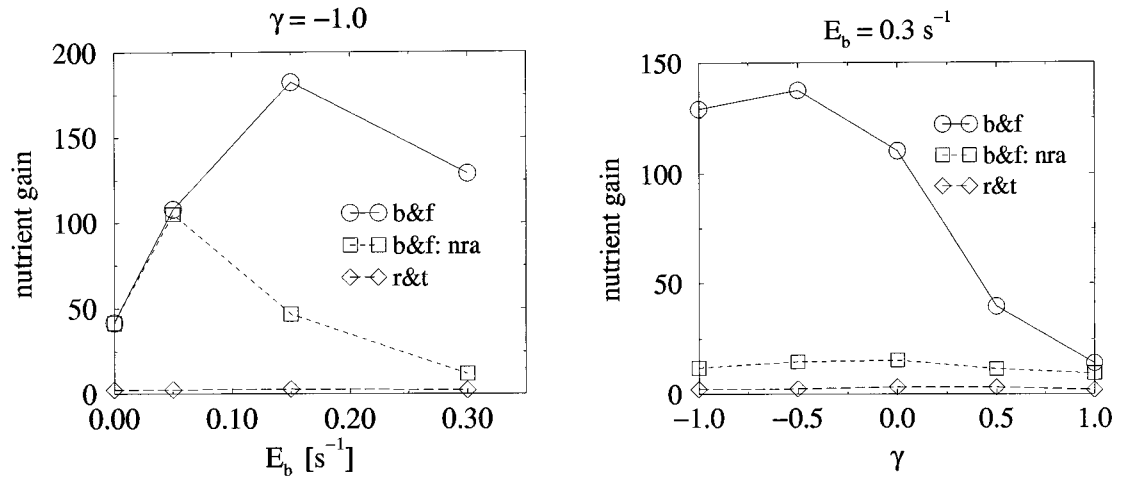

FIGURE 6 The nutrient gain of a bacterium as a function of the shear strength E_b with fixed γ (*A*), and as a function of the shear symmetry γ with fixed E_b (*B*). The back-and-forth (b&f) strategy with and without rotational advection (b&f: nra) is compared to the run-and-tumble strategy (r&t). The rotational diffusion coefficient D_r is set at 0.062 rad^2 s^{-1}, while the bacterial speed is, by default, 150 μm s^{-1}.

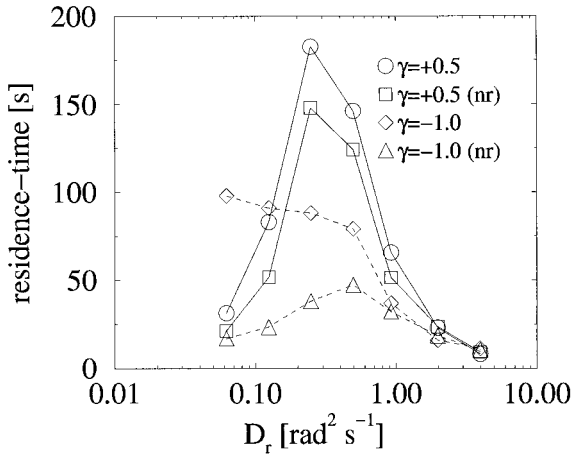

FIGURE 7 The residence time of a back-and-forth bacterium as a function of its size represented by the rotational diffusion coefficient D_r. The shear rate E_b is set at 0.3 s^{-1}, and a bacterial speed of 150 μm s^{-1} is used. Two different shear patterns ($\gamma = -1$ and $\gamma = 0.5$) are shown. Simulations without rotational advection are labeled (nr). A logarithmic scale is used to better represent the relation to the bacterial size. D_r varies from 0.062 rad^2 s^{-1} to 4.0 rad^2 s^{-1}, corresponding approximately to spheres of radii 1 μm and 0.25 μm, respectively.

dence time ranges from a few seconds to ~3 min, depending on D_r and γ, which is on the order of the Kolmogorov time. Much longer residence times would not be meaningful because of the intermittent nature of the flow (Jiménez, 1997).

The normalized exudation rate F_* was set at 1140 μm s throughout these simulations. This is the upper limit for F_* (Bowen et al., 1993) and corresponds to a regime in which bacteria can respond well to the change in the nutrient concentrations at hand. Because the chemotaxis parameters of marine bacteria have not been determined so far, the assumption that they will lie in a range where the bacteria can be effective seems natural. But the numerical values of the nutrient gain and the residence time do depend on F_*. For a test, F_* was set at 570 μm s, while F, D, and α were kept fixed at the values of Table 1, and the other parameters are set at the default values. According to Eq. 19 the half-saturation constant K_D is doubled. The residence time is then reduced by almost a factor of 2 under these conditions. Thus the chemotaxis parameters are important for quantitative results. The spirit of this work is to compare the back-and-forth with the run-and-tumble strategy under otherwise identical conditions. For that purpose qualitative answers suffice.

All of the results so far were obtained in a flow field without vorticity, but a general velocity gradient tensor will also consist of a rotational part. We performed test simulations with shear and vorticity of strength E_b, with the vorticity in the direction of the eigenvector of the intermediate eigenvalue of the rate-of-strain tensor. This direction is again suggested by numerical studies (Ashurst et al., 1987). The simulation was then run for the back-and-forth strategy with and without vorticity, using the default values for E_b, v, and D_r. We assumed the nutrient distribution to be determined by diffusion only. The change in residence time with the inclusion of vorticity is most pronounced for $\gamma = \pm 0.5$, but in both cases the residence time increased when the flow also had a rotational component (Table 2). The bacterium, under strong flow conditions, can stay close to an alga, independently of whether the flow has a rotational part. However, the residence time, as well as the nutrient gain, depends weakly on the antisymmetrical part of the flow.

In another test the random nature of the velocity field was modeled by allowing the shear symmetry factor γ to make a random walk confined between -1 and 1. The time scale of this Wiener process was defined by setting the diffusion rate equal to E_b, leading to significant changes in the form of the flow within the Kolmogorov time. This is certainly not a realistic model for the random nature of the velocity field, but it allows us to investigate the validity of the static approximation. Using the default values for all parameters and a nutrient distribution determined by diffusion only, the nutrient uptake with a random γ was compared to the average nutrient uptake from five runs with fixed γ (-1, -0.5, 0, 0.5, 1). The nutrient uptake for the stochastic γ was insignificant (~1% reduction). A similar stochastic treatment of E_b led to the same conclusion. These simple tests suggest that a more realistic stochastic treatment of the flow field is equivalent to an averaging over the static flow field, while the qualitative behavior would be the same.

CONCLUSIONS

We have compared two different swimming strategies for marine bacteria. For the back-and-forth strategy it is crucial that the bacterial heading is changed by rotational advection and rotational diffusion. This enables the bacteria to stay in the nutrient patch for times on the order of minutes and allows for a high nutrient uptake. In contrast, no significant nutrient gain, compared to that of a passive bacterium, is found for the run-and-tumble strategy.

The global picture emerging from our study is that marine bacteria rely on the symmetrical part of the flow to bring them toward a nutrient patch. A back-and-forth strategy is then employed to maximize the time spent within a high nutrient region. In this light motility in marine bacteria has a control function rather than the approach function found in enteric bacteria, and, as such, both flow and motility appear to be required for marine bacteria to cluster around a nutrient source.

As the reader by no doubt has become aware, the present simulations have some weaknesses. The most serious are probably that we have not treated vorticity or nonstationary

TABLE 2 Influence of vorticity on residence time

Shear symmetry factor γ	−1.0	−0.5	0.0	0.5	1.0
Change in residence time (%)	3	24	−2	49	−11

aspects of the flow field in detail. We believe that these problems cannot be fully overcome before the typical environment faced by microorganisms is better understood experimentally. We hope our paper will help persuade some that it is not enough to characterize the turbulence by a single number E_b, but that a more detailed description is necessary to understand the physical environment of microorganisms in the ocean.

APPENDIX: ANALYTICAL RESULTS FOR THE NUTRIENT DISTRIBUTION IN A SHEAR FLOW

The integral of Eq. 10 can be solved along the axes for $\gamma = -1$ and $\gamma = +1$. For $\gamma = -1$, the result is

$$C(x, 0, 0, t) = \frac{F}{4\pi Dx}\frac{1}{2}\left(\operatorname{erfc}\left[\sqrt{\frac{E_b a^2}{\exp[2E_b t] - 1}}\right] + \exp[E_b a^2]\operatorname{erfc}\left[\sqrt{\frac{E_b a^2}{1 - \exp[-2E_b t]}}\right]\right), \quad (21)$$

$$C(0, y, z, t) = \frac{F}{4\pi D\sqrt{y^2 + z^2}}\exp\left[-\frac{E_b}{2}b^2\right]\operatorname{erfc}\left[\sqrt{\frac{E_b}{2}b^2\frac{1 + \exp[-E_b t]}{1 - \exp[-E_b t]}}\right], \quad (22)$$

with

$$a^2 = \frac{x^2}{2D}, \quad b^2 = \frac{y^2 + z^2}{4D}, \quad (23)$$

where E_b is defined in Eq. 5 and erfc is the complement of the error function.

The steady-state distributions C are readily obtained in the limit $t \to \infty$:

$$C(x, 0, 0) = \frac{F}{4\pi Dx}\frac{1}{2}(1 + \exp[E_b a^2]\operatorname{erfc}[\sqrt{E_b a^2}]), \quad (24)$$

$$C(0, y, z) = \frac{F}{4\pi D\sqrt{y^2 + z^2}}\exp\left[-\frac{E_b}{2}b^2\right]\operatorname{erfc}\left[\sqrt{\frac{E_b}{2}b^2}\right]. \quad (25)$$

Similar expressions result for $\gamma = +1$. We only mention the steady-state distribution, which in this case is

$$C(x, y, 0) = \frac{F}{4\pi D\sqrt{x^2 + y^2}}\exp\left[\frac{E_b}{2}c^2\right]\operatorname{erfc}\left[\sqrt{\frac{E_b}{2}c^2}\right], \quad (26)$$

$$C(0, 0, z) = \frac{F}{4\pi Dz}\frac{1}{2}(\operatorname{erfc}[\sqrt{E_b d^2}] + \exp[-E_b d^2]), \quad (27)$$

with

$$c^2 = \frac{x^2 + y^2}{4D}, \quad d^2 = \frac{z^2}{2D}. \quad (28)$$

In the limit $E_b = 0$ one obtains the pure diffusion distribution as expected. It is interesting to note that for $\gamma = -1$ the distribution approaches $\frac{1}{2}(F/4\pi Dx)$ for large x. This is half of the pure diffusion distribution and is independent of the shear rate. The same result was found by an approximative analysis (Bowen and Stolzenbach, 1992).

The above results are given only along specific directions. While we were not able to give an analytical result covering the whole space, the simplest approximation for $\gamma = -1$ is

$$C(x, y, z) = \frac{F}{4\pi Dr}\frac{1}{2}(1 + \exp[E_b a^2]\operatorname{erfc}[\sqrt{E_b a^2}]) \times \exp\left[-\frac{E_b}{2}b^2\right]\operatorname{erfc}\left[\sqrt{\frac{E_b}{2}b^2}\right], \quad (29)$$

with $r = \sqrt{x^2 + y^2 + z^2}$. This expression reveals the exact results along the axes and is a reasonably good approximation for the rest of the space, as comparison with the exact numerical results have shown. A similar expression can be found for $\gamma = +1$.

The authors thank Ann Gargett for an informative discussion on turbulence in the ocean and Tim Pedley and Pete Jumars for their valuable comments on an early version of the manuscript. Thanks are due to Greg Barbara and Nick Blackburn for showing us their data on bacterial behavior. We have also benefitted from helpful discussions with Phil Austin and other members of the Crisis Point Group associated with the Peter Wall Institute for advanced studies.

This work is supported by the Swiss National Science Foundation, the Australian Research Council, the Flinders University of South Australia, and the Natural Sciences and Engineering Research Council of Canada.

REFERENCES

Ashurst, W. T., A. R. Kerstein, R. M. Kerr, and C. H. Gibson. 1987. Alignment of vorticity and scalar gradient with strain rate in simulated Navier-Stokes turbulence. *Phys. Fluids.* 30:2343–2353.

Azam, F. 1998. Microbial control of oceanic carbon flux: the plot thickens. *Science.* 280:694–696.

Baker, M. A., and C. H. Gibson. 1987. Sampling turbulence in the stratified ocean: statistical consequences of strong intermittency. *J. Phys. Oceanog.* 17:1817–1836.

Barbara, G. M., and J. G. Mitchell. 1996. Formation of 30- to 40-micrometer-thick laminations by high-speed marine bacteria in microbial mats. *Appl. Environ. Microbiol.* 62:3985–3990.

Batchelor, G. K. 1979. Mass transfer from a particle suspended in fluid with a steady linear ambient velocity distribution. *J. Fluid Mech.* 95: 369–400.

Batchelor, G. K. 1980. Mass transfer from small particles suspended in turbulent fluid. *J. Fluid Mech.* 98:609–623.

Batchelor, G. K. 1987. An Introduction to Fluid Dynamics. Cambridge University Press, Cambridge.

Berg, H. C. 1983. Random Walks in Biology. Princeton University Press, Princeton, NJ.

Berg, H. C., and D. A. Brown. 1974. Chemotaxis in *Escherichia coli* analyzed by three-dimensional tracking. *Antibiot. Chemother.* 19:55–78.

Bowen, J. D., and K. D. Stolzenbach. 1992. The concentration distribution near a continuous point source in steady homogeneous shear. *J. Fluid Mech.* 236:95–110.

Bowen, J. D., K. D. Stolzenbach, and S. W. Chisholm. 1993. Simulating bacterial clustering around phytoplankton cells in a turbulent ocean. *Limnol. Oceanog.* 38:36–51.

Brown, D. A., and H. C. Berg. 1974. Temporal stimulation of chemotaxis in *Escherichia coli. Proc. Natl. Acad. Sci. USA.* 71:1388–1392.

Denman, K. L., and A. E. Gargett. 1988. Multiple thermoclines are barriers to vertical exchange in the subarctic pacific during SUPER, May 1984. *J. Mar. Res.* 46:77–103.

Denman, K. L., and A. E. Gargett. 1995. Biological-physical interactions in the upper ocean: the role of vertical and small scale transport processes. *Annu. Rev. Fluid Mech.* 27:225–255.

Hennes, K. P., and C. A. Suttle. 1995. Direct counts of viruses in natural waters and laboratory cultures by epifluorescence microscopy. *Limnol. Oceanog.* 40:1050–1055.

Hill, P. S., A. R. M. Novell, and P. A. Jumars. 1992. Encounter rate by turbulent shear of particles similar in diameter to the Kolmogorov scale. *J. Mar. Res.* 50:643–668.

Jackson, G. A. 1987. Simulating chemosensory responses of marine microorganisms. *Limnol. Oceanog.* 32:1253–1266.

Jiménez, J. 1997. Oceanic turbulence at millimeter scales. *Sci. Mar.* 61: 47–56.

Konopka, P. 1995. Analytical Gaussian solutions for anisotropic diffusion in a linear shear flow. *J. Non-Equilib. Thermodyn.* 20:78–91.

Lazier, J. R. N., and K. H. Mann. 1989. Turbulence and the diffusive layers around small organism. *Deep-Sea Res.* 36:1721–1733.

Mitchell, J. G. 1991. The influence of cell size on marine bacterial motility and energetics. *Microb. Ecol.* 22:227–238.

Mitchell, J. G., A. Okubo, and J. A. Fuhrman. 1985. Microzones surrounding phytoplankton form the basis for a stratified marine microbial ecosystem. *Nature.* 316:58–59.

Mitchell, J. G., L. Pearson, and S. Dillon. 1996. Clustering of marine bacteria in seawater enrichments. *Appl. Environ. Microbiol.* 62: 3716–3721.

Pedley, T. J., and J. O. Kessler. 1992. Hydrodynamic phenomena in suspensions of swimming microorganisms. *Annu. Rev. Fluid Mech.* 34:313–359.

Sournia, A. 1978. Phytoplankton Manual: Monographs on Oceanographic Methodology, Vol. 6. UNESCO, Paris. 337.